AD NUMBER
AD455675
LIMITATION CHANGES

TO:

Approved for public release; distribution is unlimited.

FROM:

Distribution authorized to U.S. Gov't. agencies and their contractors; Administrative/Operational Use; SEP 1964. Other requests shall be referred to Ballistic Research Lab., Aberdeen Proving Ground, MD.

AUTHORITY
ARRADCOM ltr 20 Feb 1981

AD 455675

FENSE DOCUMENTATION CENTER

FOR

CIENTIFIC AND TECHNICAL INFORMATION

CAMERON STATION ALEXANDRIA. VIRGINIA

BRL

REPORT
NO. 1263

THE TRANSIENT RESPONSE OF
GELATIN TARGETS TO PROJECTILE IMPACTS

By J. T. Frasier

SEPTEMBER 1964
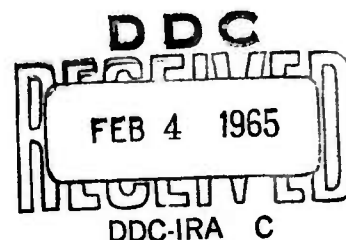
U. S. ARMY MATERIEL COMMAND
BALLISTIC RESEARCH LABORATORIES
ABERDEEN PROVING GROUND, MARYLAND

Destroy this report when it is no longer needed.
Do not return it to the originator.

BALLISTIC RESEARCH LABORATORIES

REPORT NO. 1263

SEPTEMBER 1964

THE TRANSIENT RESPONSE OF
GELATIN TARGETS TO PROJECTILE IMPACTS

J. T. Frasier

Exterior Ballistics Laboratory

ABERDEEN PROVING GROUND, MARYLAND

BALLISTIC RESEARCH LABORATORIES

REPORT NO. 1263

JTFrasier/ilm
Aberdeen Proving Ground, Md.
September 1964

THE TRANSIENT RESPONSE OF
GELATIN TARGETS TO PROJECTILE IMPACTS

ABSTRACT

This report presents results obtained in the course of an investigation of the transient response of gelatin targets to projectile impacts at 1.37 kilometers per second. The report has two main sections. The first describes the experimental technique used to gather transient response data for the targets, and presents and discusses the test results. The second section is devoted to development of a data reduction method through which observed particle velocity-time response for the elastic deformation of a target may be analyzed to yield load-time response. Some of the present data are reduced using this method and the indication is that a useful supplement to the observed results has been achieved.

TABLE OF CONTENTS

I. INTRODUCTION

For several years an experimental program has been conducted in the Ballistic Research Laboratories (BRL) to study the transient response of semi-infinite targets to projectile impact. The intent of the program is to provide data that will assist in the formulation and evaluation of theoretical analyses of the hypervelocity impact problem[1*]. Accordingly, an induction-wire technique has been developed to record the velocity-time response of particles situated on the (deformation) axis-of-symmetry of normally impacted targets[2,3,4**]. The technique has been used extensively with wax blocks. Collected data were reduced to supply the speed of propagation of the shock front generated in the targets by impacting pellets, as well as the peak particle velocity, normal stress, and density ratio at the front. To date, however, no use has been made of the observed velocity histories subsequent to initial particle disturbance by the shock. Significant advantages would be gained if methods were available to reduce these data in terms of stress levels, strains, and deformation rates. Toward this end, a reduction technique is developed in this report for the case of elastic target deformations. Attention was restricted to the elastic case to provide a basis for study of more complex situations involving permanent deformations.

The reduction technique to be presented is applicable to a diversity of problems involving high intensity, short duration loads with axial or spherical symmetry. It is most clearly given in terms of specific data. Hence, the development here will be with reference to experimental results obtained in an investigation for the Hugoniot of a gelatinous target material. At the impact velocity used (1.37 kilometers per second) the targets displayed a large region of elastic behavior; therefore, the data are convenient for present purposes.

---

* Superscript numbers denote references found on page 37.

** The technique is applicable only to electrically nonconducting targets.

The report is arranged in two sections. The first describes the experimental method and presents the data along with its reduction to provide the characteristic features of the front of the target disturbance. This includes the Hugoniot of the material. The second section develops and applies the method for analyzing the elastic response of the targets.

II. THE EXPERIMENT

1. Description of Experiment and Presentation of Results

The experiments consisted of firing 0.30-caliber cylindrical projectiles 3/8 inches in length at 9-inch-cube target blocks. The gun was smooth bore. The experimental data collected were velocity-time records for particles on the axis-of-symmetry of the deformation field generated by the normal impact of the projectile on the target face. The projectile material was ethocel (projectile mass, approximately 0.5 gram) while the target blocks were gelatin (see Appendix A for the casting and instrumentation procedures of this particular material). The impact velocity for all data given here was nominally 1.37 kilometers per second. The particle velocity-time data were obtained by use of the imbedded wire technique developed initially for use in studies in wax[*]. Adaptation for use with the present material presented no practical difficulties.

In order to have a sufficiently complete description of the axial response of the targets, and to get the necessary data to determine the Hugoniot curve, the wire particle-velocity monitors were placed at six stations along the axis-of-symmetry of the targets. A spacing of 1.27 centimeters between wires was used, with the first wire located 1.27 centimeters from the target face (Figure 1). A representative set of oscilloscope records from a firing is shown in Figure 2. These records provide a velocity history of the particles at each station, and time-of-arrival data for the front initiated by the impact. With the arrival data, the average velocity of propagation between wires is given by

---

[*] Details of this experimental technique have been presented and discussed previously. The reader is referred to References 2, 3, and 4 for details.

8

1.27 CM   3.81 CM   6.35 CM

2.54 CM   5.08 CM   7.62 CM

PROJECTILE

$\vec{V}$
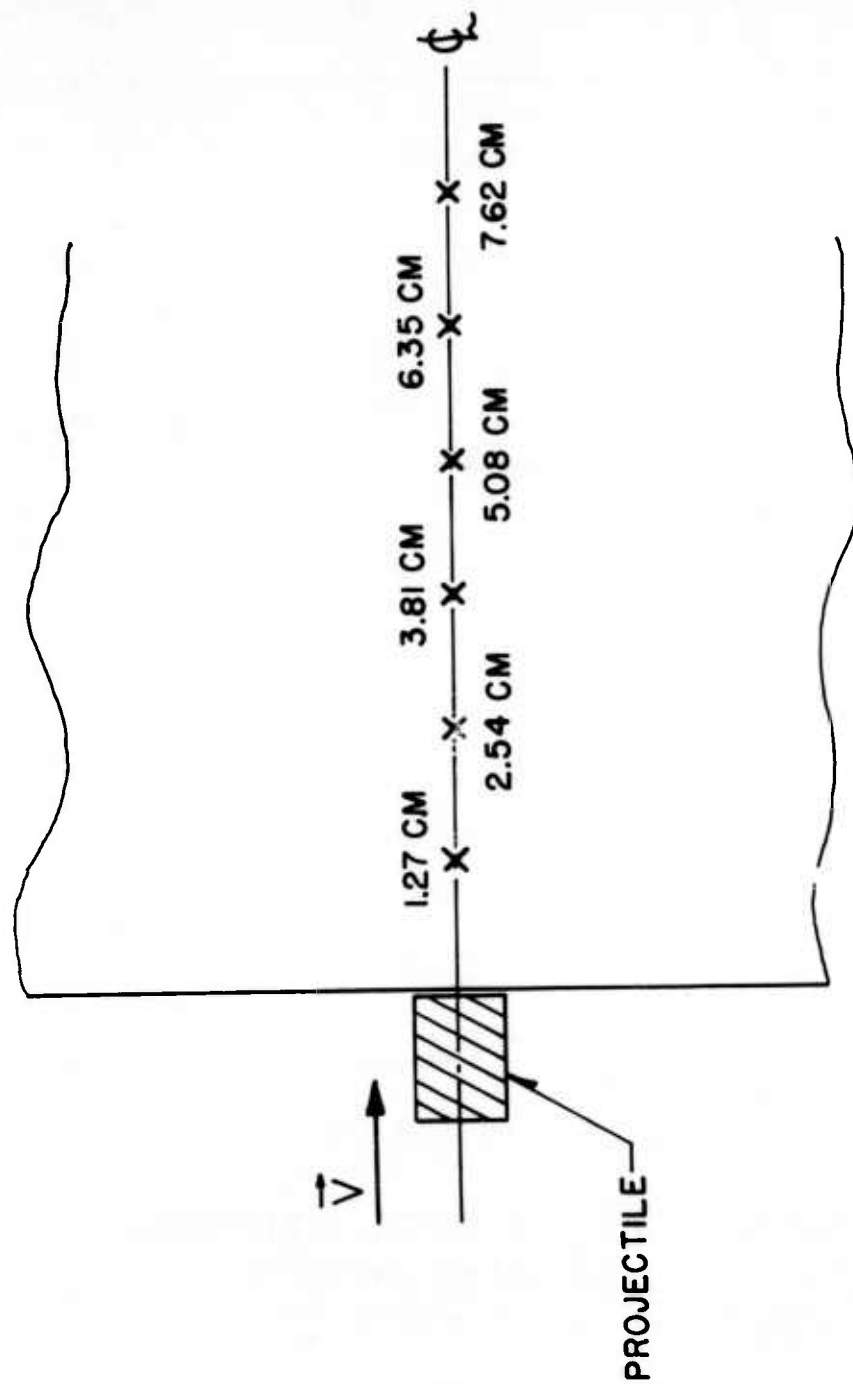
A SECTION THROUGH THE AXIS OF SYMMETRY OF
THE TARGET SHOWING THE LOCATIONS OF THE PARTICLES
MONITORED BY THE WIRE PICK-UPS

Fig I

$U_R = 34.2 \dfrac{M/SEC}{CM} \uparrow$ ——— 2.54 CM

$U_R = 34.2 \dfrac{M/SEC}{CM} \uparrow$ ——— 1.27 CM

TIME, 5 μ SEC/CM ➝

$U_R = 17.1 \dfrac{M/SEC}{CM} \uparrow$ ——— 5.08 CM

$U_R = 17.1 \dfrac{M/SEC}{CM} \uparrow$ ——— 3.81 CM

TIME, 5 μ SEC/CM ➝

$U_R = 8.55 \dfrac{M/SEC}{CM} \uparrow$ ——— 7.62 CM

$U_R = 8.55 \dfrac{M/SEC}{CM} \uparrow$ ——— 6.35 CM

TIME, 10 μ SEC/CM ➝
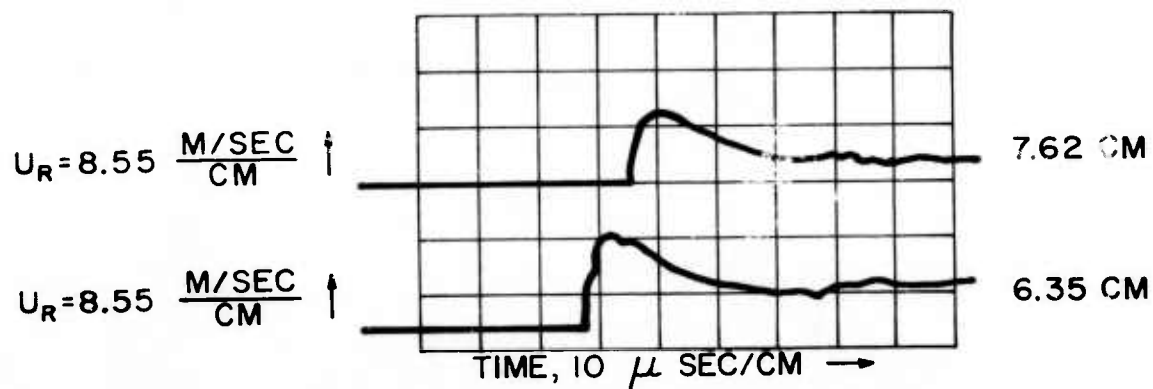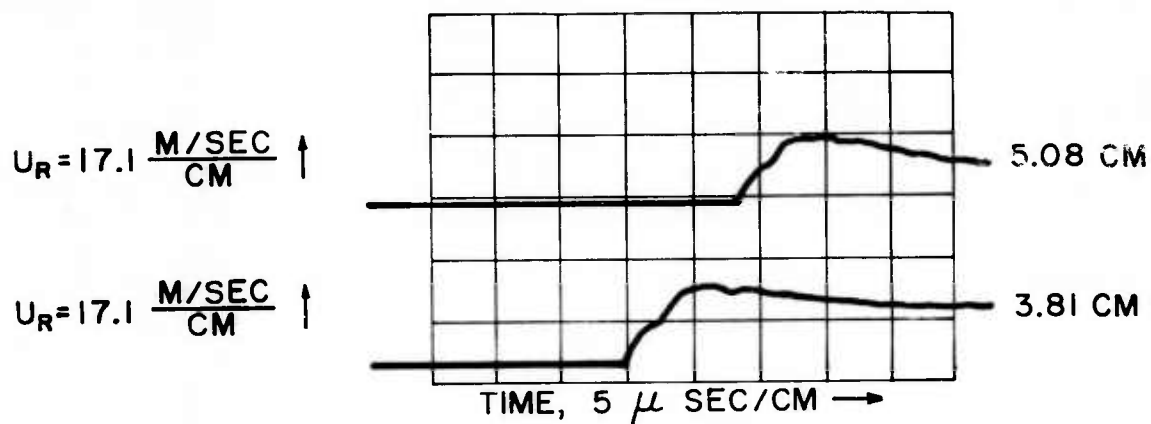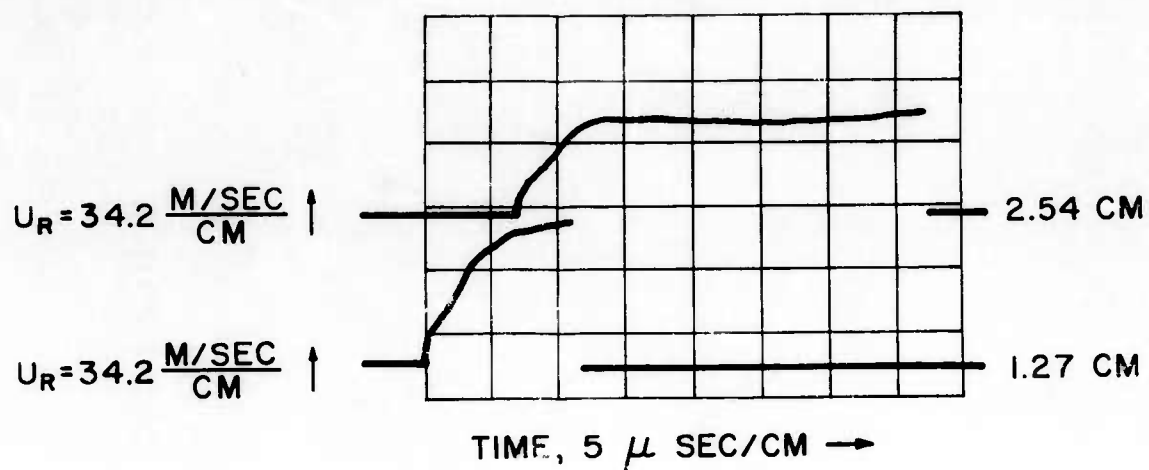
A REPRESENTATIVE SET OF DATA RECORDS
FOR AN ETHOCEL-GELATIN IMPACT.
IMPACT VELOCITY 1.37 KM/SEC.

Fig 2

$$U = \frac{D}{T} ,$$

<div align="right">(II-1)</div>

where D is the wire spacing, millimeters, and T is the travel time between wires, microseconds. For the ethocel-gelatin impacts studied here, the velocity of propagation data are shown in Figure 3 as a plot against distance from the point of impact. Data are shown only for travel times taken from the records of individual oscilloscopes, i.e., for 1.27 to 2.54 centimeters; 3.81 to 5.08 centimeters; and 6.35 to 7.62 centimeters. Although all three oscilloscopes are simultaneously triggered at impact, zero-time reference from photograph-to-photograph is not sufficiently well determined to provide accurate elapsed times.

The behavior demonstrated by the data of Figure 3 is qualitatively as expected. The front of the disturbance propagates with decreasing velocity as it penetrates the target block, asymptotically reaching a value of 1.55 kilometers per second. This occurs by the time the front arrives at the 3.81-centimeter station. The upward trend of the curve between 5 and 7 centimeters was a repeatable characteristic of these particular tests and was found not to be an instrumentation error. However, results of tests not reported here show this trend is not to be expected to continue. It is most probably due to a weak nonlinear characteristic of the target material. The velocity of 1.55 kilometers per second may be taken to be the elastic dilatational wave velocity, C_D.

Figure 4 presents the maximum particle velocity in the deformation field just behind the advancing front of the disturbance. These data are gotten by noting the peak electromotive force on the oscilloscope records of the type shown in Figure 2. The voltage is directly proportional to the particle velocity[3]. The scatter in results is due to variation in impact velocity and other round-to-round irregularities. It is more evident for the particle velocity, u, than for the velocity of propagation, U, shown in Figure 3 since the former is a more sensitive function of conditions at impact.
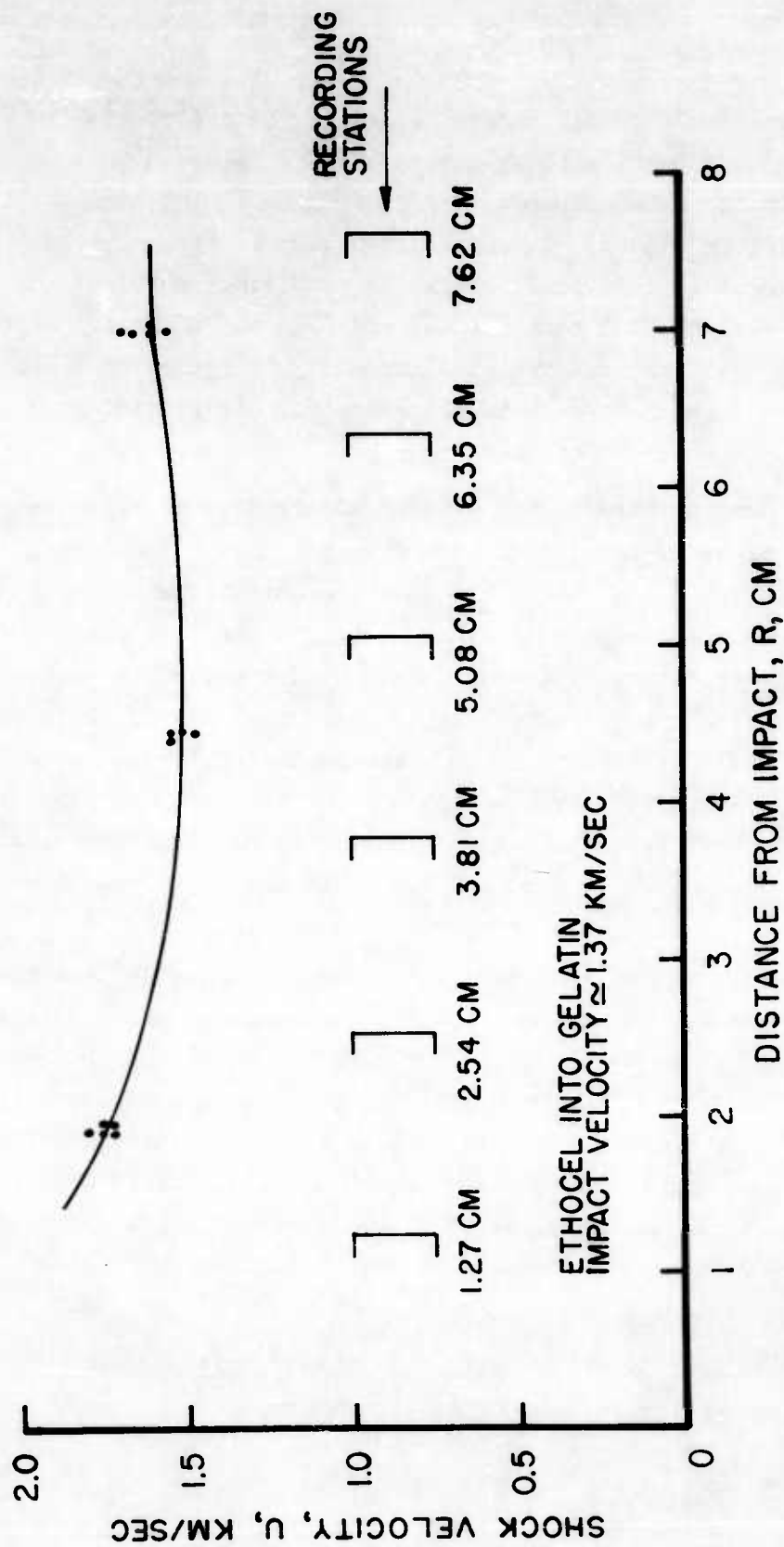
VELOCITY OF PROPAGATION OF THE DISTURBANCE
FRONT AS A FUNCTION OF DISTANCE FROM THE IMPACT POINT

Fig 3
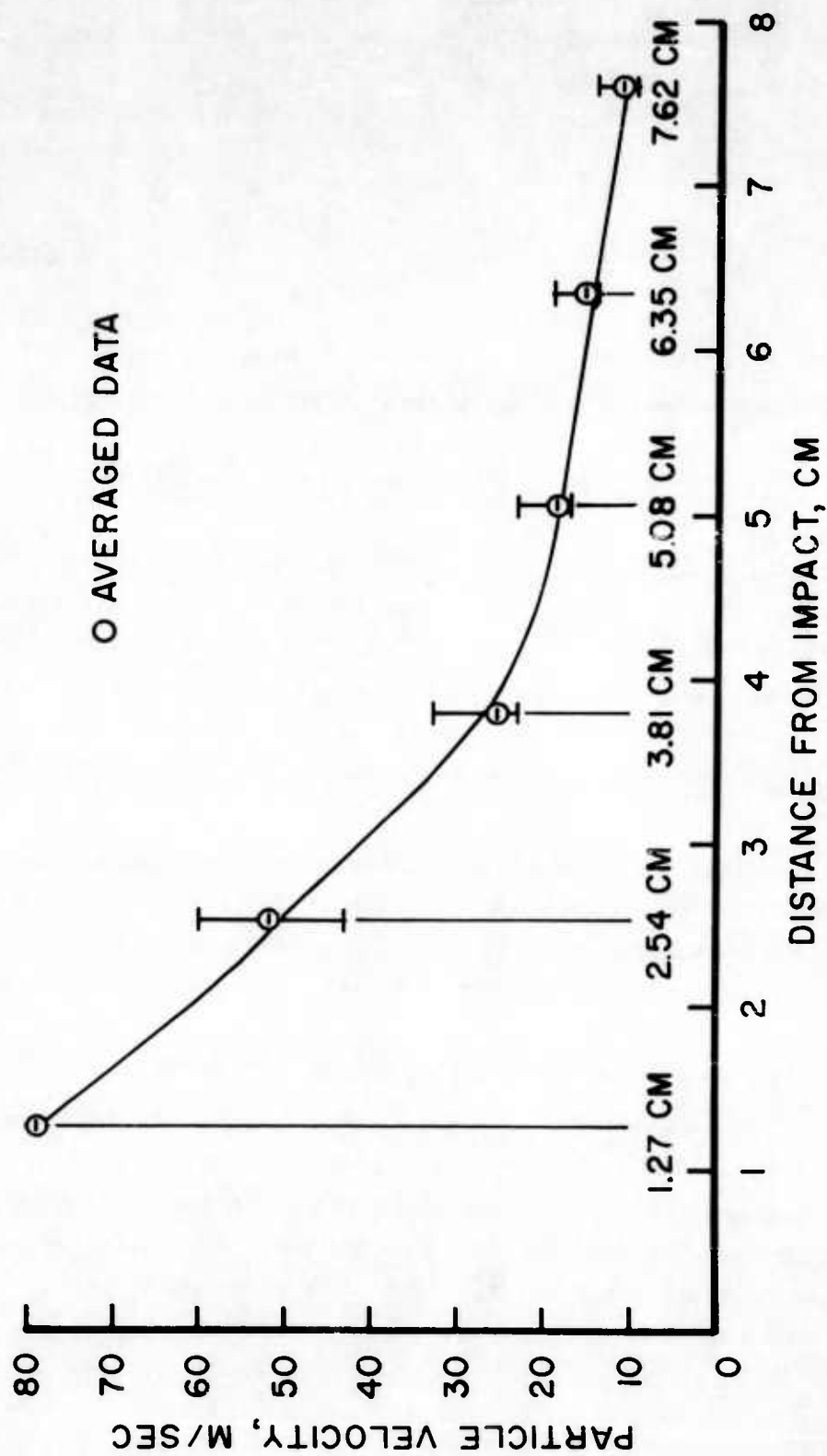
MAXIMUM PARTICLE VELOCITY VS DISTANCE FROM IMPACT FOR ETHOCEL–GELATIN AT 1.37 KM/SEC

Fig 4

13

The velocity of propagation, U, and maximum particle velocity behind the disturbance front, u, given in Figures 3 and 4, respectively, are sufficient information to determine the Hugoniot curve for the target material. The data points for this curve are obtained through use of the conservation relations

$$\sigma_R{}^* = -\rho_o\, Uu \qquad\qquad\qquad (\text{II-2})$$

$$\frac{\tau}{\tau_o} = \frac{U - u}{U}\,, \qquad\qquad\qquad (\text{II-3})$$

where $\sigma_R{}^*$ = maximum radial stress at the front of the disturbance
ρ_o = undisturbed density of the target material, 1.02 grams per cubic centimeters
$\dfrac{\tau}{\tau_o} = \dfrac{\rho_o}{\rho}$ = specific volume ratio at the front of the disturbance.

Figure 5 is a plot of the Hugoniot curve obtained from the data shown in Figures 3 and 4. Up to a stress level of 4×10^8 dynes per square centimeter, the data are well represented by a straight line whose slope gives a value for U of 1.55 kilometers per second. Above this load level, the curve shows a slight but definite increase in slope. This was to be expected from the behavior of U at points closer to the target face than 3.81 centimeters.

To extend the Hugoniot curve to stress levels greater than achieved here will require further experiments. It is worth noting, however, that the target's major constituent is water. Gross differences between the Hugoniots for the two materials are not to be expected. Within the load range covered here, this is evidenced by noting that the propagation velocity, U, for water is about 1.45 kilometers per second.

The terminal appearance of the targets provides a useful supplement to the transient data. A hemispherical region of intense cracking and fracture exists around the impact point. The radius of this region is 2.5 to 3.0 centimeters. A few isolated fracture surfaces usually extend to depths of 5.0 centimeters; however, there is no other evidence of
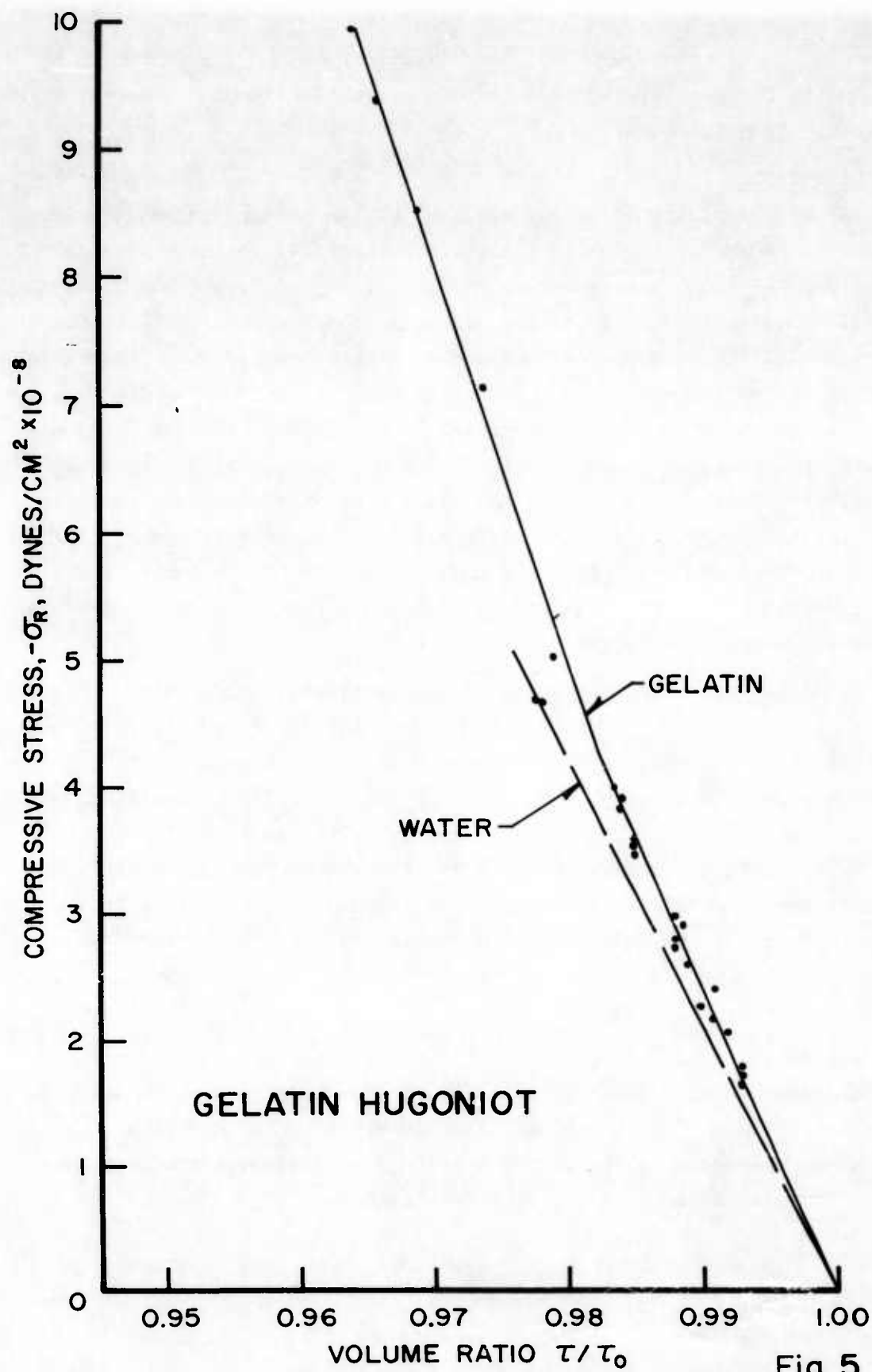
GELATIN HUGONIOT

Fig 5

permanent deformation beyond 3.0 centimeters from the target face. Hence, the indication is that the targets behave elastically past a depth of roughly 3.5 centimeters.

2. Discussion

A brief description of the response of the targets is now possible. This will be useful in the analysis of the particle velocity records. The pertinent results are given by Figures 2, 3, 4, and 5, and the terminal target appearance. The impacting cylinder produces (and sustains for short period) an intense load pulse that propagates into the target. As this proceeds, its amplitude attenuates with a corresponding decrease in the velocity of propagation. Eventually, at a depth of about 3.5 centimeters, the pulse is reduced to the level of elastic deformations and the signal thereafter propagates at the elastic dilatational wave velocity. The kinetic and potential energy deposited in the material near the impact point produces continued deformation and fracture of the target for a considerable period after passage of the shock front. No details of this process are provided by the present data.

The specific characteristics of the particle velocity-time behavior are shown by the records in Figure 2. From the impact point, only the positions at 3.81 centimeters and greater are of interest as this is where elastic deformations occur. Response of the particles is qualitatively the same at each station. The material is undisturbed until arrival of the front which is signaled by a rapid rise in the particle velocity. A peak is attained in approximately 6 microseconds. Afterwards, in about 20 microseconds, the velocity decays to an appearant asymptotic value. Actually, this is the beginning of a very gentle decrease to zero velocity that lasts several hundred microseconds.

Station-to-station attenuation in pulse intensity is evidenced by the decrease in peak particle velocity plotted in Figure 4. A similar attenuation exists in the asymptotic value reached by the particle velocity after the peak. The latter decreases with distance from impact approximately as the inverse square of distance.

16

The rapid rise in particle velocity with the arrival of the disturbance front indicates the front has the nature of a shock wave. However, the resolution of measurement is adequate to show distinct structure within the shock; that is, a definite rise time (6 microseconds) to maximum velocity is evident, as is a strongly damped high frequency (250 kilocycles) oscillation during the initial rise. This oscillation produces, in most cases, a stepped appearance to the response. Through examination of the pickup and monitoring circuitry shows this oscillating behavior is not electronic in origin. It may be reasonably presumed to be a characteristic of the target response to the conditions imposed by impact.

III. ANALYSIS OF VELOCITY RECORDS

1. Preliminary Assumptions

The aim of this analysis is to use the available particle velocity-time records to deduce further characteristics of the target's elastic behavior, e.g., stresses, deformation rates, etc. Two assumptions are necessary to obtain this information. The first is that at the positions and times of interest the response is linearly elastic. The stipulation of linearity presumes the material obeys Hooke's law in the elastic region, that deformations are small, and that time effects on the elastic behavior are negligible. The magnitude of the deformations may be checked a posteriori; however, other deviations from classic elastic behavior are not so easily ascertained without extensive material testing. This does not seem necessary as it may be noted that the behavior demonstrated by Figure 3 does not indicate any strong nonlinear effects.

The second assumption is that along the axis of symmetry the target response depends only weakly on the coordinate θ (see Figure 6) and, therefore, may be considered spherically symmetric. This assumption, in conjunction with the one of elastic behavior, has been used by other investigators[6] in the study of axially symmetric problems with high-intensity, short duration loads. Data were interpreted by comparison with analytical solutions to specific problems. In contrast, the intent here is to employ the assumptions to develop a direct method of data reduction.

17
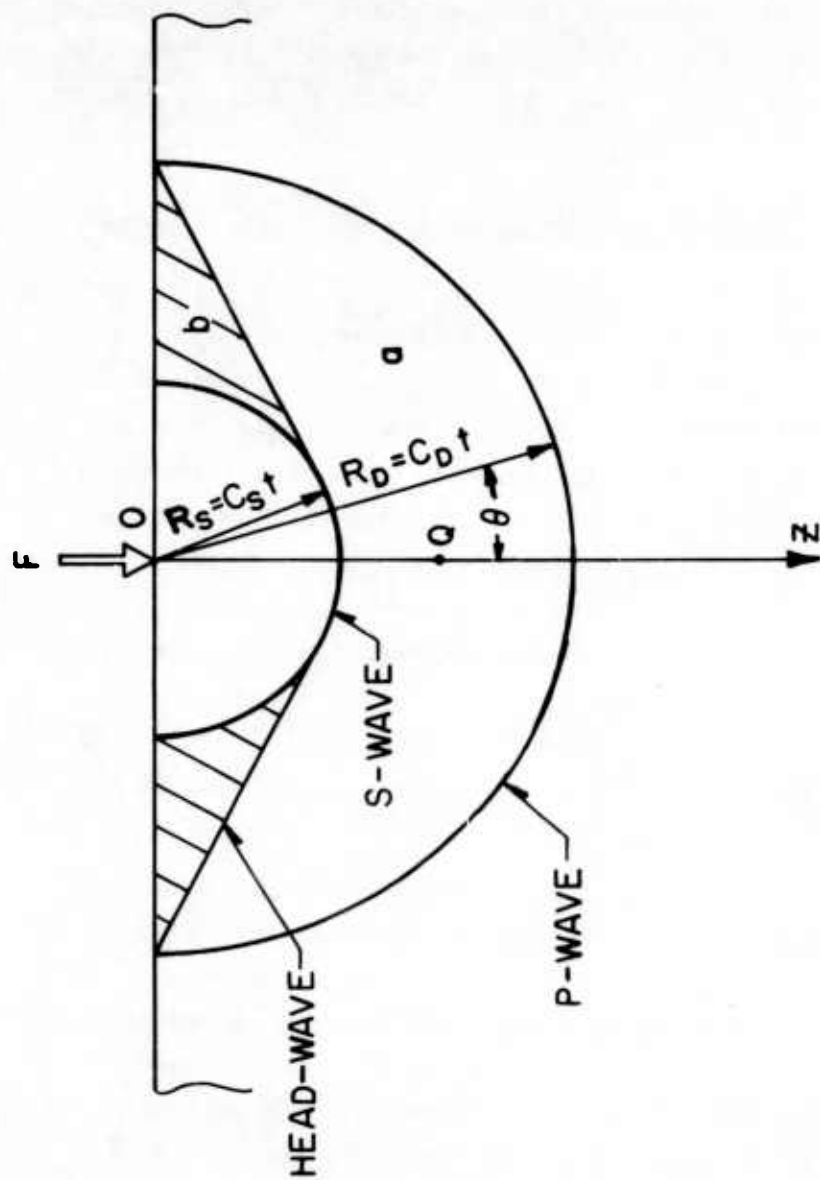
WAVE STRUCTURE FOR AN IMPULSIVE LOAD APPLIED
NORMAL TO THE SURFACE OF A SEMI-INFINITE SOLID

Fig 6a

18
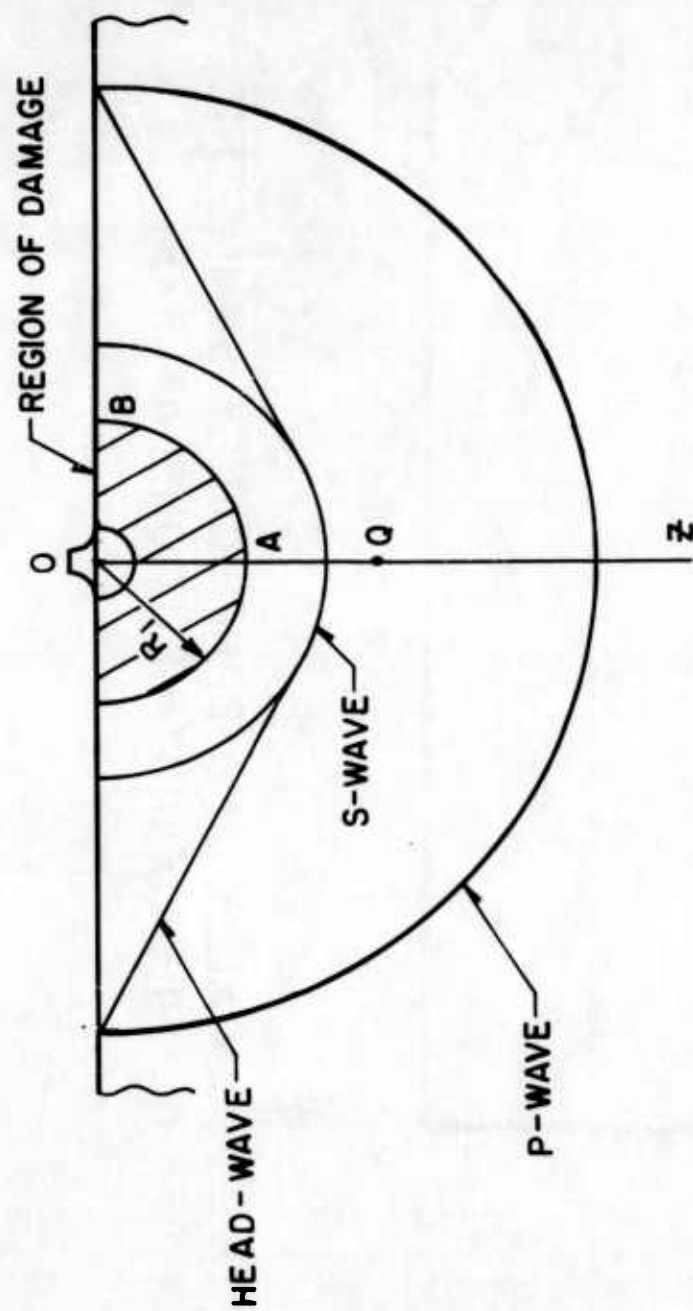
ASSUMED WAVE STRUCTURE

Fig 6b

19

The assumption of spherical symmetry results in considerable simplifications in the analysis of data; however, certain of its limitations must be kept in mind. An immediate implication is that no rotational (shear) disturbances are present in the deformation field. However, a general feature of elastic disturbances involving axial symmetry and concentrated loads is the presence of both shear and head waves following a forerunning dilatational wave. An analysis neglecting their presence can be used only so long as the deformations are reasonably assumed free of rotational disturbance. The time interval for which this is the case may be estimated by reference to Figure 6a, (a meridian plane representation of the wave pattern associated with an impulsive load F normally applied to the surface of a semi-infinite elastic solid[8]). Shown are the fronts of the dilatational, shear, and head waves initiated by application of the load at time t = 0. The disturbance in region "a" is dilatational while that in "b" is a combined dilatational and shear. A typical particle, Q, on the axis-of-symmetry OZ is undisturbed until arrival of the P-wave. Between this arrival and arrival of the S-wave, the deformation at Q is irrotational. The elapsed time between P and S arrivals and the time for which the spherically symmetric representation might be valid, therefore, is

$$T = \overline{OQ} \left(\frac{1}{C_S} - \frac{1}{C_D} \right) , \qquad \text{(III-1)}$$

where C_S is the velocity of shear waves, and C_D is the velocity of dilatational waves. Applying this representation to the present case, the formula given by Equation (III-1) serves to estimate the time interval for which an analysis based on spherical symmetry may be applied. For the gelatin, $C_D = 1.55$ kilometers per second while C_S may be taken to be roughly $C_S = 0.3$ kilometer per second[*]; therefore, with $\overline{OQ} = 3.8$ centimeters, Equation (III-1) gives

$$T \simeq 3.8(33 - 6) = 102 \ \mu sec.$$

_____

[*] This results from an assumed value for Poisson's ratio, ν, of 0.48.

21

This indicates the spherically symmetric assumption may be used without concern for effects of the shear wave for about 100 microseconds at the 3.81-centimeter station and proportionally longer for the succeeding stations[*]. In the following, no attempt will be made to analyze data records for more than 30 microseconds after arrival of the dilatational wave.

A further comment with regard to shear-wave effects must be made. In Figure 6b, a representation more nearly depicting the real situation than in Figure 6a is shown. Elastic behavior holds outside the shaded region defined by $R = R_1$; inside, combined effects of strong nonlinearity, plastic behavior, and bifurcation are anticipated. The response within $R = R_1$ defines the boundary conditions for the elastic region. It is to be noted that the previous considerations include the implicit assumption that these boundary conditions generate a P and a S-wave structure similar to that shown in Figure 6a. No direct verification of this is available.

It is recalled that the assumption of spherical symmetry was taken on the basis of weak dependence on θ of the target response along its axis of symmetry. Some justification of this is desirable even though it is plausible. Also, inquiry should be made into the adequacy of a spherically symmetric representation of the weakly θ-dependent situation. These are considered in turn.

Direct experimental or analytical evidence is not available to justify the assumption of weak θ-dependence. However, recourse is made to investigations of two related problems, the results of which indicate the assumed behavior. The first is that of Rae and Kirchner[7] and concerns the initial stages of the process of hypervelocity impact. For this problem, they have concluded θ-dependence of the deformation field on the symmetry axis is weak and that a spherically symmetric analysis adequately represents the axial behavior. The second result is the elastic solution available for a point normal impulsive force applied to the surface of a

---

[*] T is quite large owing to the gelatin having a Poisson' ratio of nearly 0.5. For more common values, the interval T will be considerably reduced.

semi-infinite solid. Here, it is found that the θ-distribution of ampli-
tude coefficients for the P-wave (see Reference 8) is weakly θ-dependent.
These two problems bracket the current one in the severity of the loading
conditions imposed at the body surface. Their demonstration of the weak
θ-dependence lends substance to assuming it here.

Final consideration is given to the adequacy of the spherically
symmetric solution to represent the weakly θ-dependent problem. Interest
is confined to distances from the impact point that are only several times
greater than R_1, the boundary of the damaged region. Figures 6b and 6c
represent the problem. The latter figure gives a comparison of θ-
independent and θ-dependent conditions on $R = R_1$. At $θ = 0$, $R = R_1$, they
are identical and therefore both present acceptable solutions. The ques-
tion is whether this continues for $R > R_1(θ = 0)$. The affirmative is seen
to hold, provided R and the time t are not too large, since the response
at a typical point Q is an integral of the effects produced by the loading
over the entire surface $R = R_1$. The effect produced by a load applied at
$θ = π/2$ is felt at Q at a time later (in proportion to the distances
$\overline{AQ}$, $\overline{BQ}$) than one simultaneously applied at $θ = 0$. Furthermore, the mag-
nitude of the response produced by loading at B is attenuated more
severely than a corresponding signal from A due to $\overline{BQ}$ being greater than
$\overline{AQ}$.

2. Analysis

It is well known that elastic disturbances possessing spherical
symmetry may be represented by a single potential function satisfying the
spherical-wave equation, that is,

$$\phi(R,t) = \frac{F(\tau)}{R} , \qquad (III-2)$$

where $\tau = t - \dfrac{R}{C_D}$

C_D = velocity of elastic dilatational waves

t = time

R = distance from the center of symmetry.

The single displacement component, u_R, is given by

$$u_R = \frac{\partial \phi}{\partial R} \,, \tag{III-3}$$

and the stress components, σ_R, σ_θ, are provided by Hooke's law as

$$\sigma_R = \frac{E}{(1 + \nu)(1 - 2\nu)} \left[(1 - \nu) \frac{\partial u_R}{\partial R} + 2\nu \frac{u_R}{R} \right] \,, \tag{III-4}$$

$$\sigma_\theta = \frac{E}{(1 + \nu)(1 - 2\nu)} \left[\frac{u_R}{R} + \nu \frac{\partial u_R}{\partial R} \right] \,, \tag{III-5}$$

where E and ν are Young's modulus and Poisson's ratio, respectively. The corresponding strains are

$$\epsilon_R = \frac{\partial u_R}{\partial R} \tag{III-6}$$

$$\epsilon_\theta = \frac{u_R}{R} \,. \tag{III-7}$$

Within the framework of Equations (III-2) through (III-7), it is seen that the assigned task of determining characteristics of the deformation or load fields, in addition to the observed velocity history at a specific axial station, reduces to determination of the function $F(\tau)$ [Equation (III-2)]. Two approaches to this problem are to be developed here. The first involves empirical construction of a function, $F(\tau)$, that adequately represents the velocity history at a specific particle position $R = R_1$. This function is then used to determine the stress and velocity behavior within the elastic region of the target. The second approach involves a graphical analysis of the individual records at each station, $R = R^*$, to provide the function $F(t - R^*/C_D)$ for these stations separately. With this method, it is possible to evaluate the desired response characteristics at each station from the particle velocity history at that station.

24

The first of the two approaches is appealing owing to the analytical compactness with which it represents the target deformation. Although guidance is provided by known solutions to dynamic problems having spherical symmetry, a major drawback to the method is the effort required to establish the "adequate" representation of the available data record. The second approach does not possess this difficulty and has the attribute of being direct and devoid of ambiguity. It is the more appropriate of the two for reduction of data from several stations, as in the present case, or for interpreting large amounts of data. The two methods are considered separately below.

a. Construction of a Function $F(\tau)$ to Represent an Observed Velocity-Time Record. The characteristic behavior of the velocity-time records has been discussed previously. For purposes of analysis attention is restricted here to interpretation of the records from a single test, the round shown in Figure 2. Also, selection of the function F is based on the data obtained at a single station, $R = 5.08$ centimeters. The adequacy of the selected representation may then be checked by determining whether it satisfactorily portrays the velocity history at the other data stations.

Enumeration of all the details associated with selecting the specific function used to represent the velocity record would be difficult. Briefly, it was noted that the impulsive nature of the projectile loading was in many ways similar to a uniform load suddenly applied to the interior of a spherical cavity. The response to such a loading situation consists of exponentially damped circular functions. With this guide, a satisfactory function F was found to be of the form

$$F = F_1(\tau) + F_2(\tau) , \qquad (III\text{-}8)$$

where $F_1(\tau) = -A_1\, e^{-\gamma_1 \tau} \sin(\flat_1\, \tau + \alpha_1)$,

$$F_2(\tau) = -A_2 \left\{ (\sin \alpha_2)\tau + \frac{e^{-\gamma_2 \tau}}{(\gamma_2^{\,2} + \flat_2^{\,2})} \left[\gamma_2 \sin(\flat_2\, \tau + \alpha_2) \right.\right.$$

$$\left.\left. + \flat_2 \cos(\flat_2\, \tau + \alpha_2) \right] \right\}$$

$$F_1 = F_2 \equiv 0 \text{ for } \tau < 0 ,$$

and

$$\cot \alpha_1 = \frac{\gamma_1}{\flat_1} .$$

The function F_1 describes the high frequency oscillations while F_2 describes the gross behavior of the deformation response. From Equation (III-2), it is to be noted that $\tau = 0$ represents arrival of the disturbance at any station, R.

Applying Equation (III-8) to Equations (III-2) and (III-3), the velocity history is

$$v = v_1 + v_2 = \frac{\partial}{\partial t} \left[\frac{\partial}{\partial R} \left(\frac{F_1 + F_2}{R} \right) \right] ,$$

with

$$\frac{v_1}{A_1} = -\frac{1}{R}\, e^{-\gamma_1 \tau} \left\{ \left[\left(\frac{\gamma_1^{\,2} - \flat_1^{\,2}}{C_D} \right)^2 + \left(\frac{2\gamma_1\, \flat_1}{C_D} \right)^2 \right]^{1/2} \cos(\flat_1\, \tau + \alpha_1 + \beta_1) \right.$$

$$\left. + \frac{1}{R} \left[(\gamma_1^{\,2} + \flat_1^{\,2}) \right]^{1/2} \sin \flat_1\, \tau \right\} \qquad\qquad \text{(III-9)}$$

$$\frac{v_2}{A_2} = \frac{\sin \alpha_2}{R^2} - \frac{1}{R}\, e^{-\gamma_2 \tau} \left[\left(\frac{1}{R} - \frac{\gamma_2}{C_D} \right)^2 + \left(\frac{\flat_2}{C_D} \right)^2 \right]^{1/2} \sin(\flat_2\, \tau + \alpha_2 + \beta_2)$$

where
$$\tan \beta_1 = \frac{\gamma_1^2 - \rho_1^2}{2\gamma_1 \rho_1}$$

$$\tan \beta_2 = \frac{\rho_2/c_D}{(1/R - \gamma_2/c_D)} \ .$$

A restriction placed on Equation (III-9) is that v be zero for $\tau = 0$. This leads to the relation

$$A_1 \left[(\gamma_1^2 - \rho_1^2)\sin \alpha_1 - 2\gamma_1 \rho_1 \cos \alpha_1 \right]$$

$$+ A_2 \left[\gamma_2 \sin \alpha_2 - \rho_2 \cos \alpha_2 \right] = 0 \ . \qquad \text{(III-10)}$$

The parameters in Equation (III-9) that define a specific profile of velocity versus time are γ_1, γ_2, ρ_1 and ρ_2. The γ's are decay factors while the ρ's establish frequency of oscillation. The constants A_1 and A_2 are amplitude coefficients for the two functions v_1 and v_2. Appropriate values of the profile factors for the R = 5.08-centimeter curve of Figure 2 are:

$$\gamma_1 = 0.800 \text{ microsecond}^{-1} \ (\mu\text{sec}^{-1})$$
$$\rho_1 = 2.520 \ \mu\text{sec}^{-1}$$
$$\gamma_2 = 0.145 \ \mu\text{sec}^{-1}$$
$$\rho_2 = 0.069 \ \mu\text{sec}^{-1}.$$

Due to the rapid attenuation of v_1, the amplitude coefficient A_2 is established with sufficient accuracy by requiring $(v_2)/\text{max}$ at R = 5.08 centimeters be equal to the maximum velocity from the data record. This results in

$$A_2 = 64.5 \times 10^{-3} \text{m}^3/\text{sec}$$

which, when applied to Equation (III-10), gives

$$A_1 = 1.01 \times 10^{-10} \text{m}^3 \ .$$

27

Figure 7 is a plot of the velocity history at R = 5.08 centimeters as transcribed from the data record and as given by Equation (III-9) with the above stated values of γ_1, γ_2, etc. A good description of the actual record is seen to have been obtained except for details of the initial oscillating response. A better fit could have been obtained by further trial and error adjustment of the parameters; however, the gain achieved would not warrant the effort.

Now that the specific function F has been established to represent the velocity behavior at R = 5.08 centimeters, it may be used to evaluate other response characteristics in the target. First, a comparison should be made of the predicted and observed velocity response at the remaining data stations. This is also shown in Figure 7. The representation of actual data is seen to be excellent at all the stations for the times ($\tau \geq 0$) of interest. The agreement provides some support to the assumption of spherical symmetry. If the assumption were grossly unreasonable, marked discrepancies between the observed velocity response and that provided by F should result.

Next, the function F is used to examine further characteristics of the target response. Most significant of these are the normal stresses, σ_R, σ_θ, and the maximum shear stress $(\sigma_R - \sigma_\theta)/2$. These are obtained directly by application of Equation (III-8) to Equations (III-4) and (III-5), with the appropriate values of γ_1, γ_2, ... This has been done for the radial stress σ_R and maximum shear stress $(\sigma_R - \sigma_\theta)/2$. The results are shown in Figures 8 and 9.

The stress σ_R has a profile in time very similar to that of the velocity at each station. It quickly reaches a peak (details of the oscillatory behavior have been omitted) at about 6 microseconds and then decays to what appears to be a residual value of the order of 30 percent of the maximum stress. This shows the highly transient character of the large radial stresses imposed by the impact. The present data indicate the duration of intense loading to be about 15 microseconds. A similar circumstance may be assumed to hold in the region of damage, R < 3.81 cm (centimeters).
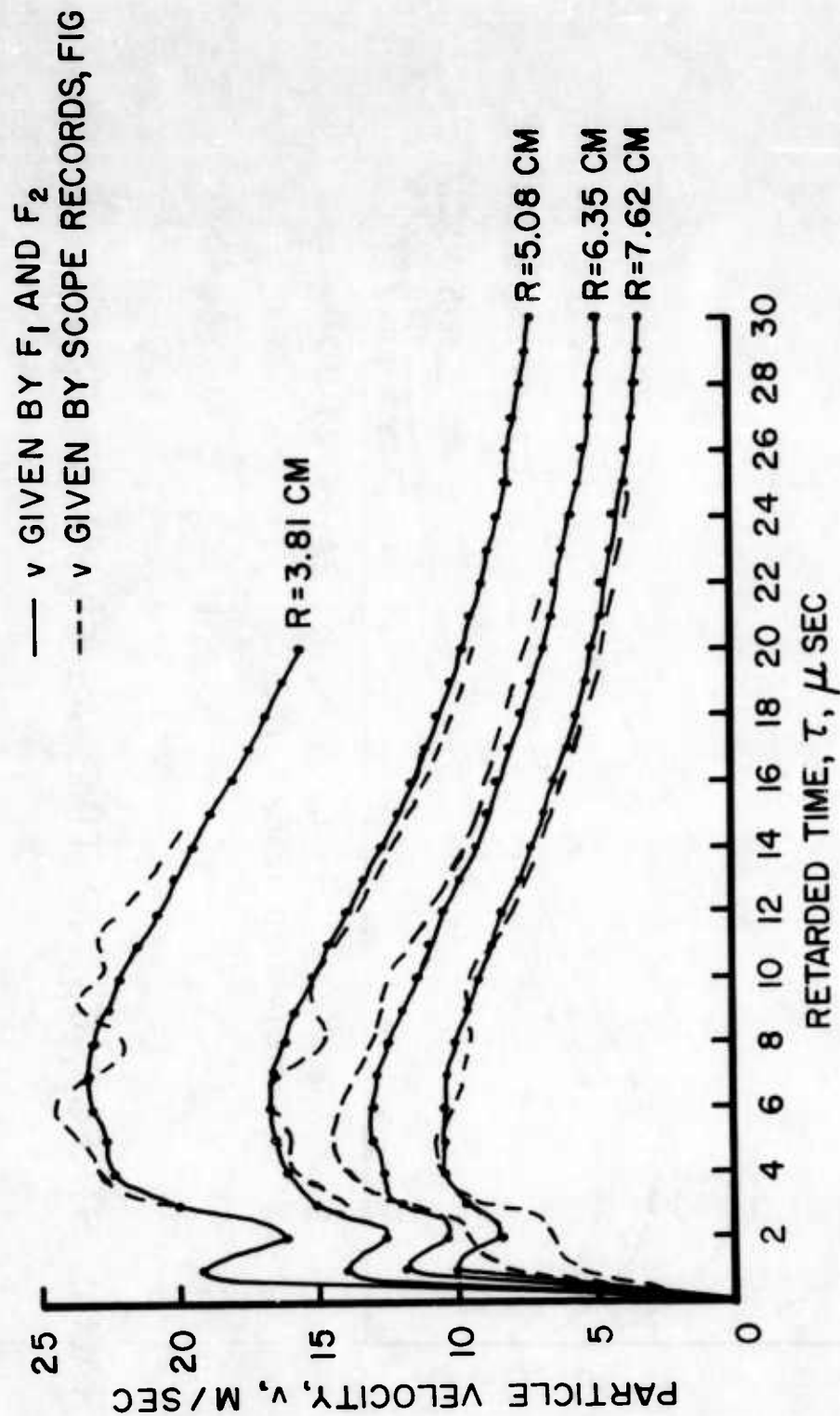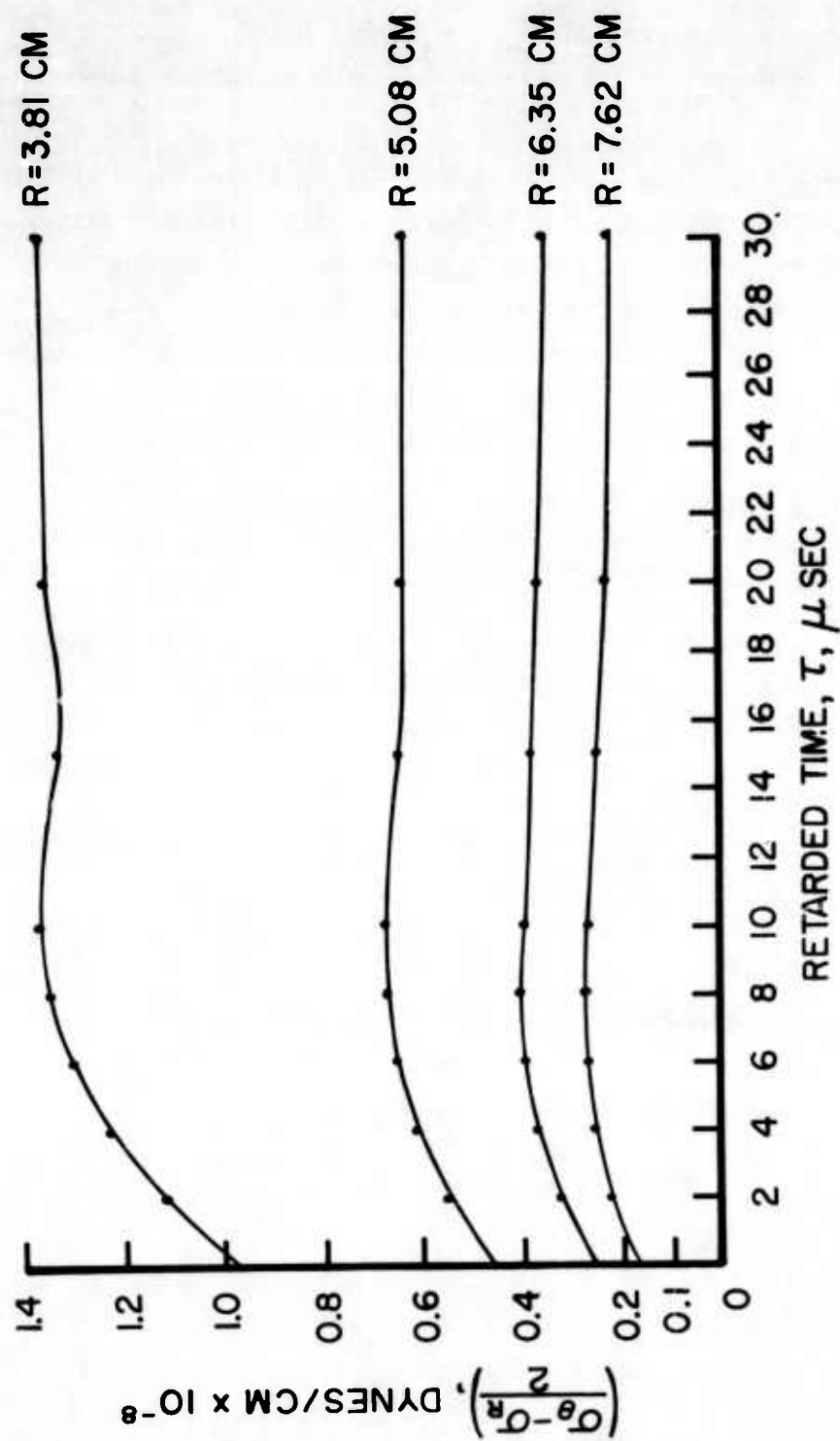
PARTICLE VELOCITY VS RETARDED TIME
AT THE MONITORING STATIONS

Fig 7

29
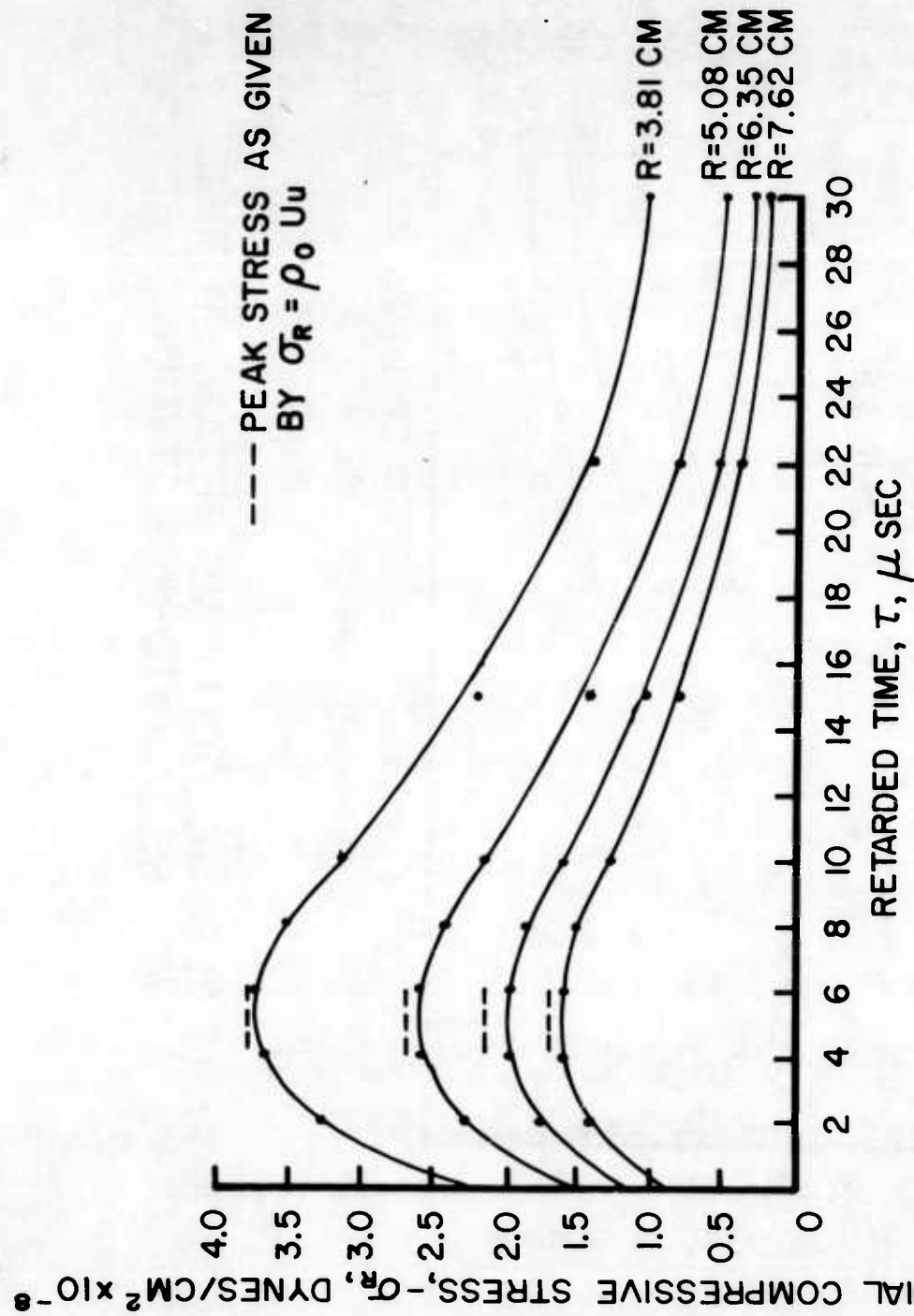
Fig 8

RADIAL STRESS, σ_R, VS TIME AS GIVEN BY $F_2(\tau)$

MAXIMUM SHEAR STRESS VS TIME AS GIVEN BY $F_2(\tau)$, $\nu = 0.48$

Fig 9

31

Figure 9 shows the behavior of $(\sigma_R - \sigma_\theta)/2$, the maximum shear stress. (Again the initial oscillatory behavior has been omitted.) Here, a qualitatively different behavior is seen than for σ_R. The shear stress reaches a peak in the same time as the radial stress, but no significant subsequent decay occurs.

b. <u>Graphical Data Reduction</u>. The method to be considered now will make use of the individual velocity-time records at each station to determine additional characteristics of the load process at these stations. With data available at several stations as in the present case, this provides a more direct means of data reduction than the previous technique. Also, it may be used when only a single data record is at hand to provide information for the region near the data station.

Advantage is taken again of the assumption of spherical symmetry. Also, use is made of the conditions $u_R = v = 0$ at $\tau = 0^*$. The result of these conditions is that $F(0) = F'(0) = F''(0) = 0$.

For a fixed station $R = R^*$, the displacement component u_R is readily obtained by a first quadrature of the data records; that is,

$$u_R(R^*,\tau) = \int_0^\tau v(R^*,\xi)d\xi, \quad \tau > 0 \qquad (III\text{-}11)$$

while $u_R(R^*,\tau) = 0;\ \tau \leq 0$. Applying this result to Equation (III-3) gives

$$\frac{F'(\tau)}{R^*C_D} + \frac{F(\tau)}{R^{*2}} = -u(R^*,\tau) , \qquad (III\text{-}12)$$

where primes denote derivatives with respect to the argument, τ. Multiplying Equation (III-12) by the integrating factor $\exp(C_D/R^*)\tau$ gives

$$\frac{d}{d\tau}\left[e^{C_D/R^*\tau} F(\tau)\right] = -(R^*C_D)e^{(C_D/R^*)\tau} u(R^*,\tau)$$

which, upon integration, yields

---

[*] This means account will be taken of the structure of the shock wave.

$$F(\tau) = e^{-(C_D/R^*)\tau}\left[-(R^*C_D)\int_0^\tau e^{(C_D/R)\xi}u(\xi)d\xi\right] . \qquad \text{(III-13)}$$

Equation (III-13) is the desired result[*]. It allows evaluation of $F(\tau)$ at any of the stations $R = R^*$ by a simple process of graphical quadratures. Consequently, any desired characteristic of the target response is immediately available through a direct process of reduction of the available data. For instance, the radial stress σ_R is given as

$$\frac{(1+\nu)(1-2\nu)}{E}\sigma_R(R^*,\tau) = -(1-\nu)\left[\frac{v(R^*,\tau)}{C_D}\right]$$

$$+ \frac{C_D}{R^{*2}}\left[e^{-(C_D/R^*)\tau}\int_0^\tau e^{(C_D/R^*)\xi}u(\xi)d\xi\right]$$

$$- (1-3\nu)\frac{u_R(R^*,\tau)}{R^*} . \qquad \text{(III-14)}$$

Evaluation of the necessary integrals in Equation (III-14), that is,

$$u_R(R^*,\tau) = \int_0^\tau v(R^*,\xi)d\xi$$

and

$$I = \int_0^\tau e^{(C_D/R^*)\xi}u_R(R^*,\xi)d\xi ,$$

has been carried out for the data shown in Figure 2 at the 3.81-, 5.08-, 6.35- and 7.52-centimeter stations. The velocity-time records were transcribed to graph paper, and a planimeter was used for integration. The results obtained are shown in Figure 10. Comparison with the results provided by the empirical choice of $F(\tau)$ yields agreement within 10 percent. The graphical method provides the details of the high frequency motion which were omitted in Figure 8.

---

[*] For a similar development involving the acoustic wave equation, see Reference 9.
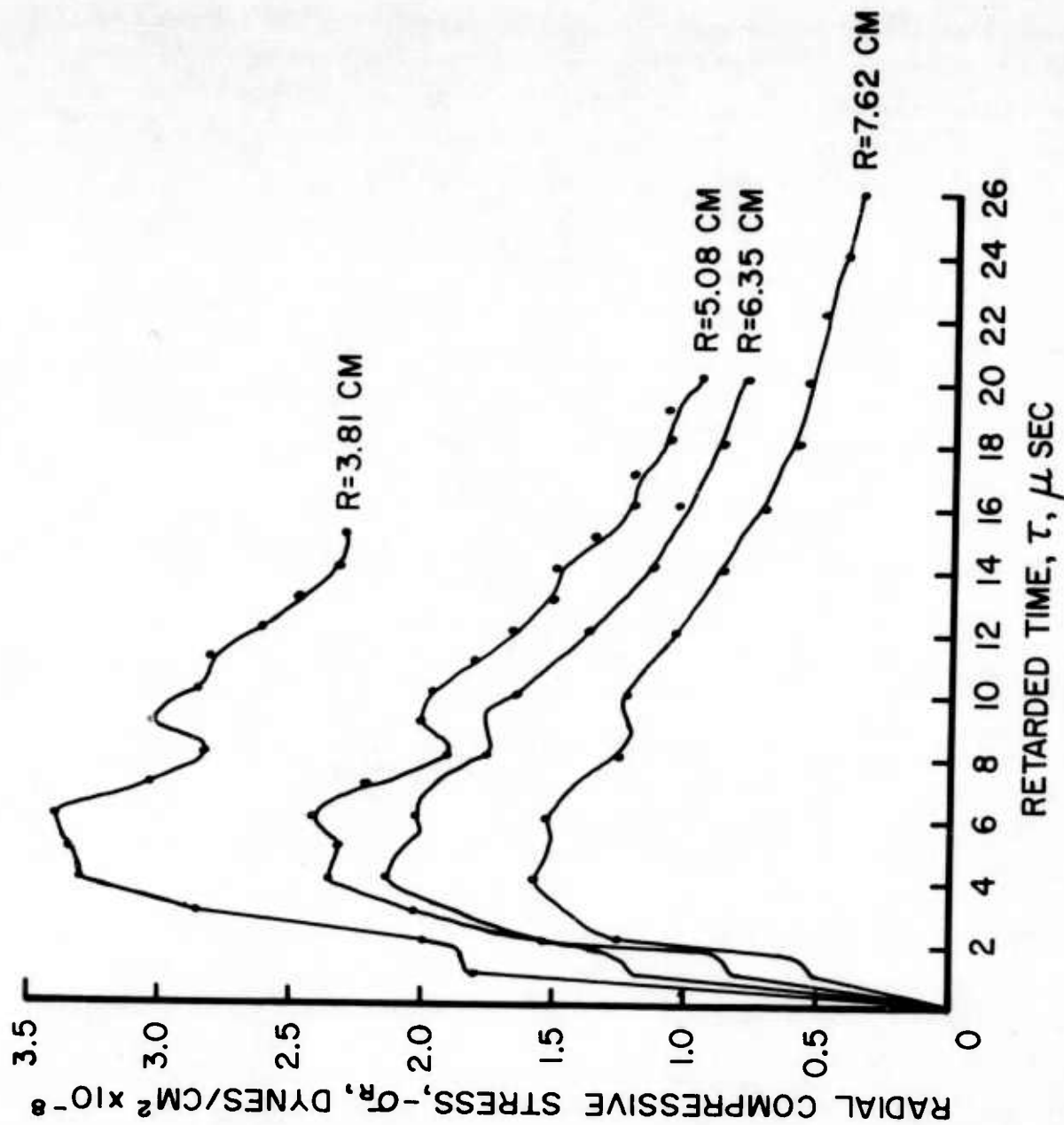
RADIAL STRESS, σ_R, AS GIVEN BY GRAPHIC EVALUATION OF $F(\tau)$ Fig 10

The most attractive feature of the graphical method is its simplicity and directness. The data at each station can be independently reduced. Also, it is to be noted that this technique provides a very useful procedure in tests where velocity-time data are available from only a single record. The functions $F(\tau)$, $F'(\tau)$ can be obtained graphically from relations such as Equations (III-13) and (III-12) at the data station. These functions may then be used for other values of R provided proper account is taken of the retarded time

$$\tau = t - \frac{R - R^*}{c_D} \, ,$$

and as long as the assumption of spherical symmetry is valid.

IV. SUMMARY AND CONCLUSIONS

1. Determination of the Hugoniot curve for the gelatin target material has been accomplished for stress levels up to 10^2 dynes per square centimeter. In this load region, the curve differs little, but distinctly, from that for water. For the load intensities covered by the present tests, this result was to be anticipated[10]. At higher load levels the same situation may be expected. Due to the practical interest for use of this particular material, a definitive determination of the Hugoniot is desirable for a more extensive range of loads than covered here. Tests are in preparation for such an extension and will be presented subsequently.

2. The curves of Figures 2, 3, and 4 summarize the characteristics of the front of the disturbance traveling into the target. The data provided furnish a detailed account of initial features of the signature imposed on the block by the projectile. A discussion of these features was given in Section II-B for the present impact situation. The ability to examine these features is significant. For many problems of practical interest involving impacts at velocities attained by service weapons, the evaluation of effects of projectile geometry is important. Appreciable understanding of these effects could be provided through systematic study of the initial transient characteristics they impose on targets.

35

3. The data analysis presented in Section III of the particle velocity-time records represents a significant extension of the basic data provided by the inductance wire pickup technique. Considerable attention has been given to justification of the necessary assumptions for making this extension. This practice seems to have been neglected by other investigators in the past. The information provided by the data analysis affords an opportunity for more detailed experimental investigation of impact phenomena than has been possible in the past. Immediate application to the study of hypervelocity impact phenomena is possible as would be its use in further studies in gelatin. It should also be pointed out that the basis of the techniques developed here is equally applicable to various problems involving high intensity loading. The most notable problems are geophysical and involve phenomena such as earthquake behavior and surface or underground explosion effects.

The foundations and application of the data reduction technique must be considered preliminary. Establishment of its accuracy and applicability can result only from further study and use.

V.   ACKNOWLEDGEMENT

The author owes a debt of gratitude to Mr. Dale M. Smith for his aid and endurance in the preparation of the target blocks.

<div align="right">J. T. FRASIER</div>

VI. REFERENCES

1. Proceedings of the Rand Symposium on High-Speed Impact. Santa Monica, California, May 1955.

   Proceedings of the Second Hypervelocity Impact Effects Symposium. U. S. Naval Research Laboratory, Washington, D. C., May 1957.

   Proceedings of the Third Symposium on Hypervelocity Impact Effects. Illinois Institute of Technology, Chicago, Illinois, October 1958.

   Proceedings of the Fourth Hypervelocity Impact Effects Symposium. Eglin Field, Florida, April 1960.

   Proceedings of the Fifth Symposium on Hypervelocity Impact. Denver, Colorado, October 1961.

   Proceedings of the Sixth Symposium on Hypervelocity Impact. Cleveland, Ohio, August 1963.

2. Frasier, J. T. Hypervelocity Impact Studies in Wax. Ballistic Research Laboratories Report No. 1124, Aberdeen Proving Ground, Maryland, February 1961.

3. Frasier, J. T. and Karpov, B. G. Hypervelocity Impact Studies in Wax. Proceedings of the Fifth Symposium on Hypervelocity Impact. Volume 1, Part 2, pages 371 - 387, Denver Colorado, October 1961.

4. Karpov, B. G. Transient Response of Wax Targets to Pellet Impact at 4 km/sec. Ballistic Research Laboratories Report No. 1226, Aberdeen Proving Ground, Maryland, October 1963.

5. Kinslow, R. Properties of Spherical Shock Waves Produced by Hypervelocity Impact. Proceedings of the Sixth Symposium on Hypervelocity Impact. Volume 2, Part 1, pages 273 - 320, Cleveland, Ohio, August 1963.

6. Goldsmith, W. and Allen, W. Graphical Representation of the Spherical Propagation of Explosive Pulses in Elastic Media. The Jour. of the Acous. Soc. of Amer., Volume 27, Number 1, pages 47 - 55, January 1955.

7. Rae, W. and Kirchner, H. Final Report on a Study of Meteoroid Impact Phenomena. CAL Report No. NAS 3-2121, February 1963.

8. Knopoff, L. and Gilbert, F. First Motion Methods in Theoretical Seismology. The Jour. of the Acous. Soc. of Amer., Volume 31, Number 9, pages 1161 - 1168, September 1959.

9. Barnes, C. and Anderson, D. V. Sound Field from a Pulsating Sphere and the Development of a Tail in Pulse Propagation. The Jour. of the Acous. Soc. of Amer., Volume 24, Number 2, page 229, March 1952.

10. Houwink, R. Elasticity, Plasticity, and Structure of Matter. Dover Publications, New York, pages 264 - 272, 1953.

APPENDIX
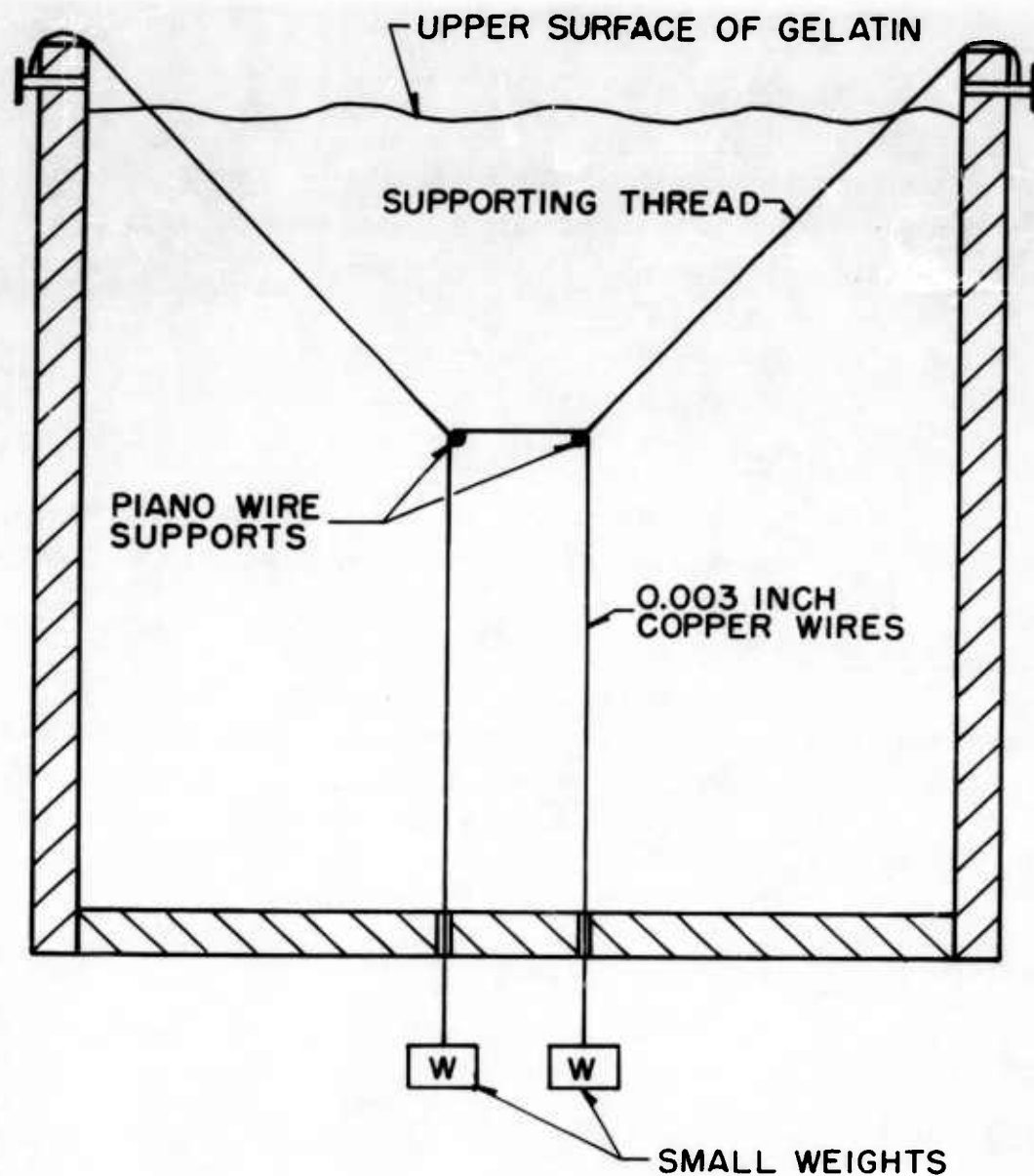
Preparation of Gelatin Targets

The target material used for these studies was a mixture of collagen[*]
and water. Generally, lots of thirty pounds were prepared in a ratio of
four parts water to one part collagen by weight. The preparation proce-
dure was as follows:

1. Collagen added to water at 180°F.

2. Constituents mixed for 3 hours at 180°F.

3. Liquid gelatin cast into 9-inch cubes and allowed to gel at
room temperature overnight.

4. Cast targets chilled to 40°F in refrigerator for 24 hours.

5. Targets removed from refrigerator and tested with a maximum
exposure of 20 minutes to room temperature of 68°F.

Method of Wire Placement

The inductance-wire-particle-velocity pickups were emplaced by means
of a rig of fine thread. A pair of taut piano wires was used to assist
in alignment of the 0.003-inch copper monitor wires. These were removed
prior to gelling of the blocks. A plane view of the arrangement is
depicted in Figure 11.

---

[*] Swift's USP Grade Pharmagel A.

UPPER SURFACE OF GELATIN

SUPPORTING THREAD

PIANO WIRE
SUPPORTS

0.003 INCH
COPPER WIRES

W   W

SMALL WEIGHTS

A CROSS SECTION OF THE TARGET MOLD
SHOWING THE METHOD OF WIRE PLACEMENT

40

Fig 11

DISTRIBUTION LIST

No. of Copies	Organization
20	Commander Defense Documentation Center ATTN: TIPCR Cameron Station Alexandria, Virginia 22314
2	Director Advanced Research Project Agency Department of Defense Washington, D. C. 20301
1	Director IDA/Weapon Systems Evaluation Group Room 1E875, The Pentagon Arlington, Virginia 20315
1	Director Defense Research and Engineering (OSD) ATTN: Director/Ordnance Washington, D. C. 20301
1	Commanding General U. S. Army Materiel Command ATTN: AMCRD-RP-B Washington, D. C. 20315
2	Commanding Officer Frankford Arsenal ATTN: Library Branch, 0270 Building 40 Philadelphia, Pa. 19137
3	Commanding Officer Picatinny Arsenal ATTN: Feltman Research and Development Labs. Dover, New Jersey 07801

No. of Copies	Organization
3	Commanding Officer Watertown Arsenal Watertown, Massachusetts 02172
1	Commanding Officer Harry Diamond Laboratories Washington 25, D. C.
2	Commanding General U. S. Army Missile Command Redstone Arsenal, Alabama 35809
1	Redstone Scientific Information Center ATTN: Chief, Document Section U. S. Army Missile Command Redstone Arsenal, Alabama 35809
1	Commanding General U. S. Army Munitions Command Dover, New Jersey 07801
1	Commanding Officer U. S. Army Materials Research Agency Watertown Arsenal Watertown, Massachusetts 02172
1	Top Secret Control Office U. S. Army Foreign Science and Technology Center Room 2621 Munitions Building Washington, D. C. 20315
1	Army Research Office 3045 Columbia Pike Arlington, Virginia

DISTRIBUTION LIST

No. of Copies	Organization	No. of Copies	Organization
1	Commanding General U. S. Army Engineering Research and Development Labs. ATTN: STINFO Branch Fort Belvoir, Virginia 22060	1	APGC (PGBAP) Eglin AFB Florida
1	Commanding Officer U. S. Army Research Office (Durham) Box CM, Duke Station Durham, North Carolina	1	APGC (PGTW) Eglin AFB Florida
2	Commander U. S. Naval Ordnance Lab. White Oak Silver Spring, Maryland 20910	1	APGC (PGTWR) Eglin AFB Florida
1	Commander U. S. Naval Ordnance Test Station ATTN: Technical Library China Lake, California 93557	1	APGC (PGTZ) Eglin AFB, Florida
2	Director U. S. Naval Research Lab. ATTN: Technical Information Division Mr. Walter Atkins Washington, D. C. 20390	1	Scientific and Technical Information Facility ATTN: NASA Representative (S-AK/DL) P. O. Box 5700 Bethesda, Maryland 20014
3	Chief, Bureau of Naval Weapons ATTN: DLI-3 Department of the Navy Washington, D. C. 20360	1	Director National Aeronautics and Space Administration Ames Research Center Moffett Field, California
2	Det #4 RTD (ATB, ATW) Eglin AFB Florida	1	Bureau of Mines ATTN: M. P. Benoy, Reports Librarian Explosives Research Laboratory 4800 Forbes Street Pittsburgh 13, Pennsylvania
1	APGC (PGTRI) Eglin AFB Florida	1	Library of Congress ATTN: Bibliograph Section Technical Information Division Reference Department Washington 25, D. C.

42

DISTRIBUTION LIST

No. of Copies	Organization	No. of Copies	Organization
1	Director U. S. Geological Survey ATTN: Mr. H. J. Moore Menlo Park, California	1	Professor J. Duffy Davision of Engineering Brown University Providence 12, Rhode Island
3	Applied Physics Laboratory The Johns Hopkins University 8621 Georgia Avenue Silver Spring, Maryland	1	Professor W. H. Hoppman II Department of Mechanics Rensselaer Polytechnic Institute Troy, New York
1	Bell Telephone Labs. Inc. Whippany, New Jersey	1	Professor Ray Kinslow Chairman, Department of Engineering Science Tennessee Polytechnic Institute Cookeville, Tennessee

1	General Motors Corporation
	Defense Systems Division,
	    Box T
	ATTN: Mr. J. W. Gehring
	Santa Barbara, California
		1	Professor R. Llorens
			Department of Mechanical
			    Engineering
			Drexel Institute of Technology
			Philadelphia 4, Pennsylvania

1	Professor James F. Bell The Johns Hopkins University Baltimore, Maryland	1	Professor Joseph Marin Department of Engineering Mechanics The Pennsylvania State University University Park, Pennsylvania
1	Professor S. Bodner Division of Engineering Brown University Providence 12, Rhode Island	1	Dr. C. H. Mok Department of Engineering Mechanics The Pennsylvania State University University Park, Pennsylvania
1	Professor P. C. Chou Department of Mechanical Engineering Drexel Institute of Technology Philadelphia 4, Pennsylvania	1	Dr. W. J. Rae Cornell Aeronautical Engineering University of Toronto Toronto, Canada

1	Professor N. Davids
	Department of Engineering
	    Mechanics
	The Pennsylvania State
	    University
	University Park, Pennsylvania
		1	Professor J. Schwaighofer
			Department of Civil Engineering
			University of Toronto
			Toronto, Canada

DISTRIBUTION LIST

No. of
Copies   Organization

1   Professor P. S. Symonds
Division of Engineering
Brown University
Providence 12, Rhode Island

1   Dr. W. Bingham
Mechanics Division
Naval Research Laboratory
Washington 25, D. C.

1   Dr. J. M. Walsh
General Atomic
P. O. Box 608
San Diego 12, California

1   Mr. A. B. J. Clark
Mechanics Division
Naval Research Laboratory
Washington 25, D. C.

1   Mr. D. Robinson
Davision of Engineering
Brown University
Providence 12, Rhode Island

1   Mr. F. S. Stepka
NASA Lewis Research Center
Cleveland, Ohio

No. of
Copies   Organization

4   Australian Group
c/o Military Attache
Australian Embassy
2001 Connecticut Avenue, N. W.
Washington, D. C. 20008

10   The Scientific Information
Officer
Defence Research Staff
British Embassy
3100 Massachusetts Avenue, N. W.
Washington, D. C. 20008

4   Defence Research Member
Canadian Joint Staff
2450 Massachusetts Avenue, N. W.
Washington. D. C. 20008

Aberdeen Proving Ground

Chief, TIB

Air Force Liaison Office
Marine Corps Liaison Office
Navy Liaison Office
CDC Liaison Office

D&PS Branch Library

AD   Accession No.   UNCLASSIFIED
Ballistic Research Laboratories, APG
THE TRANSIENT RESPONSE OF GELATIN TARGETS TO   High velocity impact -
PROJECTILE IMPACTS   Transient response
J. T. Frasier   Elastic deformation -
                                         Gelatin
BRL Report No. 1263   September 1964

RDT & E Project No. 1A222901A201
UNCLASSIFIED Report

    This report presents results obtained in the course of an investigation of the transient response of gelatin targets to projectile impacts at 1.37 kilometers per second. The report has two main sections. The first describes the experimental technique used to gather transient response data for the targets, and presents and discusses the test results. The second section is devoted to development of a data reduction method through which observed particle velocity-time response for the elastic deformation of a target may be analyzed to yield load-time response. Some of the present data are reduced using this method and the indication is that a useful supplement to the observed results has been achieved.

AD   Accession No.   UNCLASSIFIED
Ballistic Research Laboratories, APG
THE TRANSIENT RESPONSE OF GELATIN TARGETS TO   High velocity impact -
PROJECTILE IMPACTS   Transient response
J. T. Frasier   Elastic deformation -
                                         Gelatin
BRL Report No. 1263   September 1964

RDT & E Project No. 1A222901A201
UNCLASSIFIED Report

    This report presents results obtained in the course of an investigation of the transient response of gelatin targets to projectile impacts at 1.37 kilometers per second. The report has two main sections. The first describes the experimental technique used to gather transient response data for the targets, and presents and discusses the test results. The second section is devoted to development of a data reduction method through which observed particle velocity-time response for the elastic deformation of a target may be analyzed to yield load-time response. Some of the present data are reduced using this method and the indication is that a useful supplement to the observed results has been achieved.

AD _____ Accession No. _____
Ballistic Research Laboratories, APG
THE TRANSIENT RESPONSE OF GELATIN TARGETS TO
PROJECTILE IMPACTS

J. T. Frasier

High velocity impact -
Transient response
Elastic deformation -
Gelatin

BRL Report No. 1263   September 1964

RDT & E Project No. 1A222901A201
UNCLASSIFIED Report

This report presents results obtained in the course of an investigation of the transient response of gelatin targets to projectile impacts at 1.37 kilometers per second. The report has two main sections. The first describes the experimental technique used to gather transient response data for the targets, and presents and discusses the test results. The second section is devoted to development of a data reduction method through which observed particle velocity-time response for the elastic deformation of a target may be analyzed to yield load-time response. Some of the present data are reduced using this method and the indication is that a useful supplement to the observed results has been achieved.

AD _____ Accession No. _____
Ballistic Research Laboratories, APG
THE TRANSIENT RESPONSE OF GELATIN TARGETS TO
PROJECTILE IMPACTS

J. T. Frasier

High velocity impact -
Transient response
Elastic deformation -
Gelatin

BRL Report No. 1263   September 1964

RDT & E Project No. 1A222901A201
UNCLASSIFIED Report

This report presents results obtained in the course of an investigation of the transient response of gelatin targets to projectile impacts at 1.37 kilometers per second. The report has two main sections. The first describes the experimental technique used to gather transient response data for the targets, and presents and discusses the test results. The second section is devoted to development of a data reduction method through which observed particle velocity-time response for the elastic deformation of a target may be analyzed to yield load-time response. Some of the present data are reduced using this method and the indication is that a useful supplement to the observed results has been achieved.